

Supplement Information

Dual Vision-equipped Microfluidic Chip for Spatiotemporal Sequential Pick-and-Place of Oocytes

Shuzhang Liang¹, Hao Mo¹, Yuguo Dai¹, Hiroataka Sugiura¹, Satoshi Amaya¹, and Fumihito Arai^{1,*}

¹ Department of Mechanical Engineering, The University of Tokyo, Tokyo 113-8656, Japan

The PDF file includes:

Supplementary Sessions S1 to S3

Figures S1 to S20

Algorithm S1

Other Supplementary Materials for this manuscript include the following:

Video S1. Separation of objects and single release in sequence.

Video S2. Deal with unseparated case for single release.

Video S3. Pick-transport-place oocytes from one working well chip to the other working well chip.

Session S1. Camera field of view

When the camera rotates along with axis, the field of view (FOV) of camera also changes, as shown in Fig. S6 to S9. Here, we set that the camera's initial optical axis is along $-Z$ and the distance from the XY plane is L , the field of view after rotating around X or Y axis by α , as shown in Fig. S6. It gives

that camera position, and horizontal viewing angle $\theta_h = 2 \cdot \arctan \frac{w}{2f}$. The vertical viewing angle $\theta_v = 2 \cdot \arctan \frac{h}{2f}$, thus $\theta_v = 2 \cdot \arctan \left(\tan \left(\frac{\theta_h}{2} \right) \cdot \frac{h}{w} \right)$, which two viewing angles determine the

direction of the rays at the edge of the light cone of camera. Resolution aspect ratio of image of camera is $w:h = 640:480 = 4:3$, and $\theta_h = 60$ degree. The surface of the microfluidic chip is set as $Z = 0$.

When camera rotates around X axis by α , the rotation matrix is:

$$R_x(\alpha) = \begin{bmatrix} 1 & 0 & 0 \\ 0 & \cos \alpha & -\sin \alpha \\ 0 & \sin \alpha & \cos \alpha \end{bmatrix}, \quad (\text{S1})$$

When camera rotates around Y axis by α , the rotation matrix is:

$$R_y(\alpha) = \begin{bmatrix} \cos \alpha & 0 & \sin \alpha \\ 0 & 1 & 0 \\ -\sin \alpha & 0 & \cos \alpha \end{bmatrix}, \quad (\text{S2})$$

Thus, whole rotation matrix of camera is $R = R_z \cdot R_y \cdot R_x$, where, $R_z = \begin{bmatrix} 1 & 0 & 0 \\ 0 & 1 & 0 \\ 0 & 0 & 1 \end{bmatrix}$, meaning

without rotation at Z-axis.

Subsequently, we calculate FOV direction vectors. In the camera coordinate system before rotation, the four corners' directions are:

$$d = \begin{bmatrix} \tan \phi \\ \tan \psi \\ 1 \end{bmatrix}, \quad \phi \in [-\theta_h/2, \theta_h/2], \quad \psi \in [-\theta_v/2, \theta_v/2], \quad (S3)$$

The normalized direction vector is: $\hat{d} = \frac{d}{\|d\|}$. Therefore, the rotated direction vector is $\hat{d}_{rot} = R \cdot \hat{d}$.

Next, calculate the four corners' directions vector intersecting with $Z = 0$ plane (XY plane). Ray equation from camera position $C = (X_0, Y_0, Z_0)$, $Z_0 = L$ along direction $\hat{d}_{rot} = (d_x, d_y, d_z)$. Thus,

$P(t) = C + t\hat{d}_{rot} = (C_x + td_x, C_y + td_y, C_z + td_z)$. Since intersecting with $Z = 0$, thus, $C_z + td_z = 0$, then $t = -C_z/d_z = -Z_0/d_z = -L/d_z$. Therefore, the intersection coordinates are:

$$x = C_x + td_x = X_0 - \frac{Ld_x}{d_z}, \quad y = C_y + td_y = Y_0 - \frac{Ld_y}{d_z}, \quad z = 0, \quad (S4)$$

where, if $d_z = 0$, the ray is parallel to XY plane and has no intersection. The four FOV points are set $(x_i, y_i, 0)$, $i = 1, 2, 3, 4$. Thus, the width (W) and height (H) of FOV are: $W = x_{max} - x_{min}$, $H = y_{max} - y_{min}$. Setting the FOV area into two triangles, with four points A, B, C, D clockwise, the

area is: $FOV_Area = \frac{1}{2} \|(B - A) \times (C - A)\| + \frac{1}{2} \|(D - A) \times (C - A)\|$. As shown in Fig. S7, for a

camera with a 60° viewing horizontal angle, as the camera rotation angle increases from 0 to 60 degree, a larger area of the microfluidic chip can be captured.

Session S2. Timing sequence for a single control

The timing sequence for a single control is as shown in Fig. S12. These contain follows: 1. image acquisition: The miniature camera captures a frame, with a time of 33 ms per frame. 2. image processing: The received image is processed by the YOLOv5 detection model running on a RTX 3060 GPU. The average inference time per frame is around 5 ms, which includes object detection and coordinate calculation. 3. pump working: The pump response to start or stop the flow introduces with control signal. The time from pump working to medium flowing in channel measured at 270 ms, which depends on the property of pump. 4. manipulator working: the speed is set to 2 mm/s. Therefore, the total time from image capture to the initiation of a flow response in channel is approximately 308 ms. Since the step of pumps working to medium flowing in channel cost times, it can reduce time and improve real-time property by two ways: install a valve or directly install small pumps on the chip. This process ensures that the control system can effectively track and respond to oocyte movement, maintaining a stable and reliable manipulation process.

Session S3. Simulation of flow control

We simulate the flow control distribution of two pumps for picking or placing oocytes. Different input flow rates and directions are conducted, as shown in Fig. S17, and results are shown in Fig. S18. The flow can be ejected out from the tip of microfluidic chip for placing as following cases: when

pump1 infuse, pump 2 stop or infuse or withdraw under flow rate smaller than pump 1 infusing rate; when pump 1 stop, pump 2 infuse. The flow can be aspired into the tip of microfluidic chip for picking as following cases: when pump1 withdraw, pump 2 stops or withdraw or infuse under flow rate smaller than pump 1 withdrawing rate; when pump 1 stops, pump 2 withdraws. In the practice experiment of oocytes placing, pump 1 and pump 2 can cooperate for oocyte separation. Since oocytes are kept in the channel, only pump 2 is used to control single oocyte release after separation. In picking experiments, pump 1 and pump 2 can be independent or cooperate for aspiration. In the case, when the aspiration speed is faster than the camera framerate (30 frame/second), causing the inability to detect oocytes, pump 2 can be used to aspire the oocyte to the well port first which can stop the oocytes.

Supplementary Figures

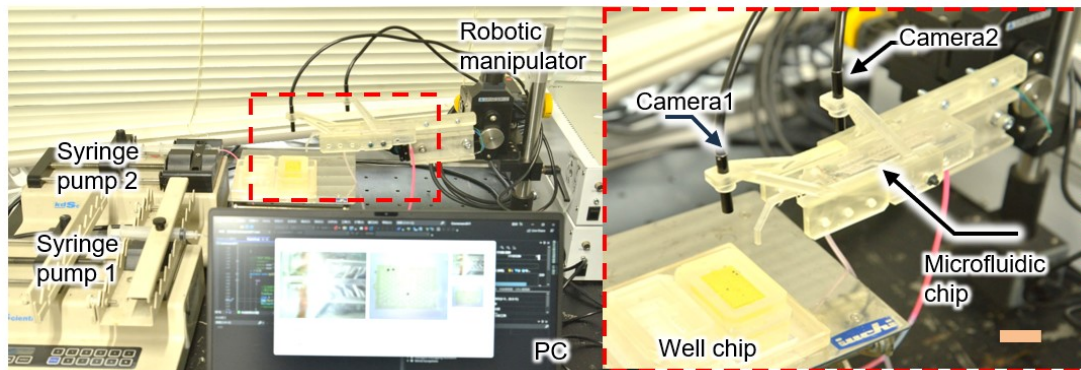


Figure S1. Real image of the system of a microfluidic chip equipped with two cameras.

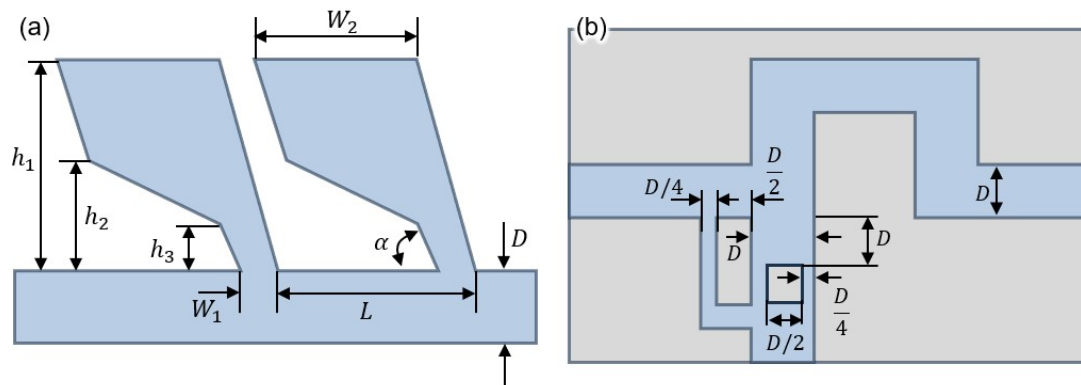


Figure S2. Parameters of the channel. (a) Main channel and branch channel, $D = 1.6 \text{ mm}$, $W_1 = 0.4 \text{ mm}$, $W_2 = 2.4 \text{ mm}$, $L = 3.2 \text{ mm}$, $\alpha = 60 \text{ deg}$, $h_1 = 3.2 \text{ mm}$, $h_2 = 1.6 \text{ mm}$, $h_3 = 0.8 \text{ mm}$. (b) Trapping well port.

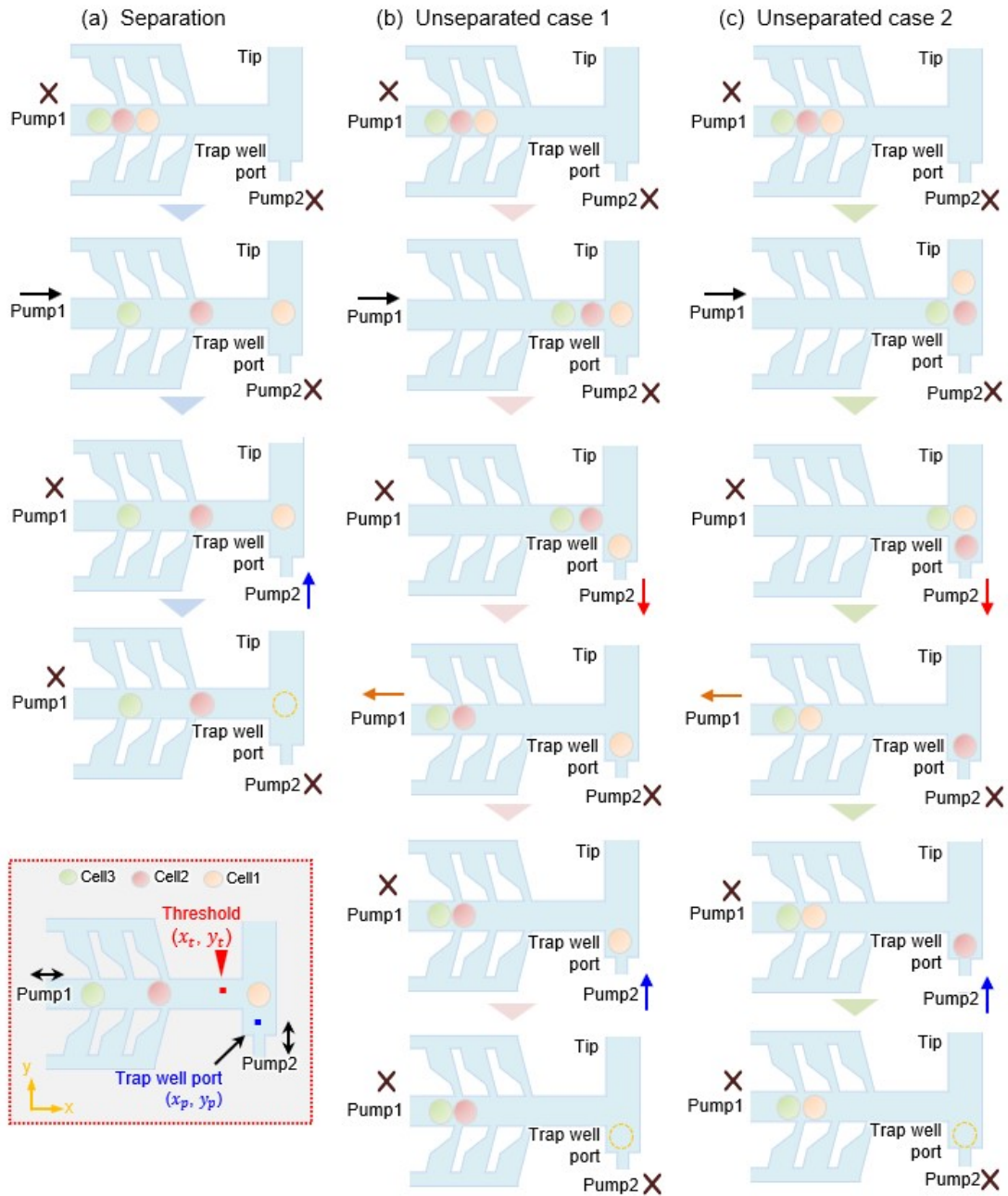


Figure S3. Based on the oocyte cells position information to determine different control effects of two pumps. (a) Separation case, pump 1 infuses then cells separation, switching to pump 2 infuse for single cell release. (b) Unseparated case 1, two cells beyond threshold position, pump 1 infuse then cells no separation, switching to pump 2 withdraw for trapping single cell, switching to pump 1 withdraw remain cells, switching to pump 2 infuse for single cell release. (c) Unseparated case 2, more than two cells beyond threshold position.

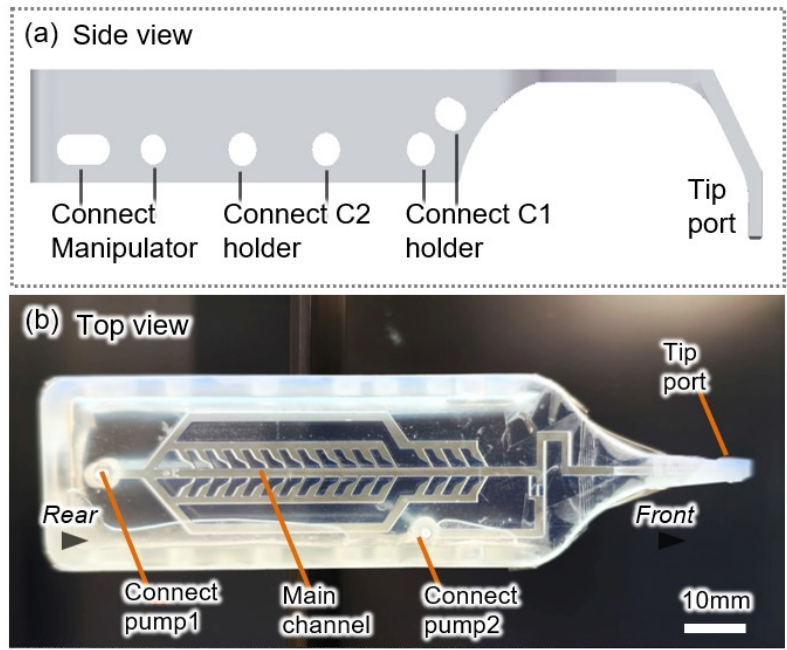


Figure S4. Microfluidic chip structure. (a) side view. (b) Top view of real image of the chip.

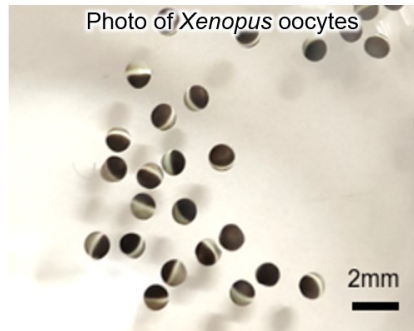


Figure S5. Real photo of *Xenopus* oocytes.

Algorithm S1. Vision detection for control robotic manipulator movements.

Input: Image I_k in well chip.

Output: Deciding the picking or placing target position (x_t, y_t) for movement of chip-on-robot.

- 1: acquire image I_k
 - 2: detect cells position $(x_{c1}, y_{c1}), (x_{c2}, y_{c2}), (x_{c3}, y_{c3}), \dots \dots$
and wells position $(x_{w1}, y_{w1}), (x_{w2}, y_{w2}), (x_{w3}, y_{w3}), \dots$
 - 3: **if picking then**
 - 4: **if user-specified then**
 - 5: $T_i\{x_t, y_t\} = U_i\{x_c, y_c\}, i = 1, 2, 3 \dots \dots$
 - 6: **if feature-specified then**
 - 7: $T_i\{x_t, y_t\} = F_i\{x_c, y_c\}, i = 1, 2, 3 \dots \dots$
 - 8: **if placing then**
 - 9: **if user-specified, then**
 - 10: $T_i\{x_t, y_t\} = U_i\{x_w, y_w\}, i = 1, 2, 3 \dots \dots$
 - 11: **if rule-specified then**
 - 12: $T_i\{x_t, y_t\} = R_i\{x_w, y_w\}, i = 1, 2, 3 \dots \dots$
 - 13: output the target position $T_i\{x_t, y_t\}$
-

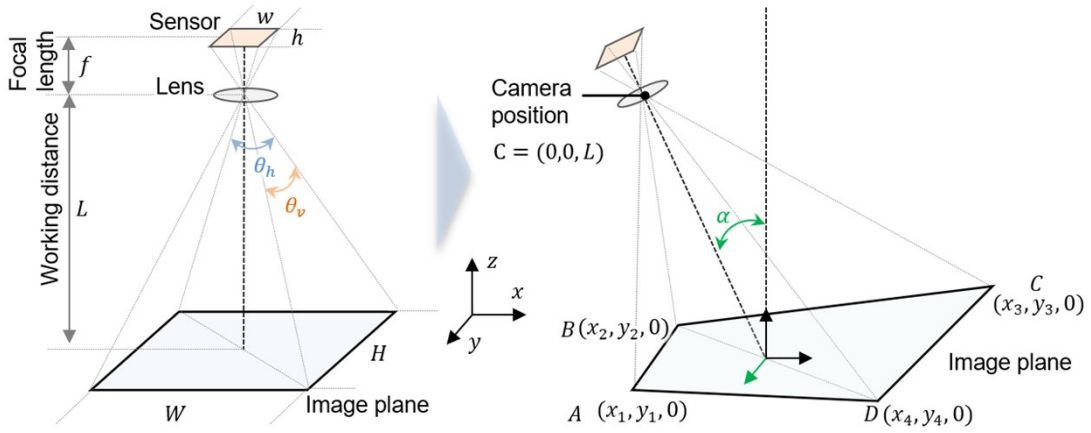


Figure S6. Scheme of camera field of view when camera rotate along with y-axis, horizontal viewing

angle $\theta_h = 2 \cdot \arctan \frac{w}{2f}$, vertical viewing angle $\theta_v = 2 \cdot \arctan \frac{h}{2f}$.

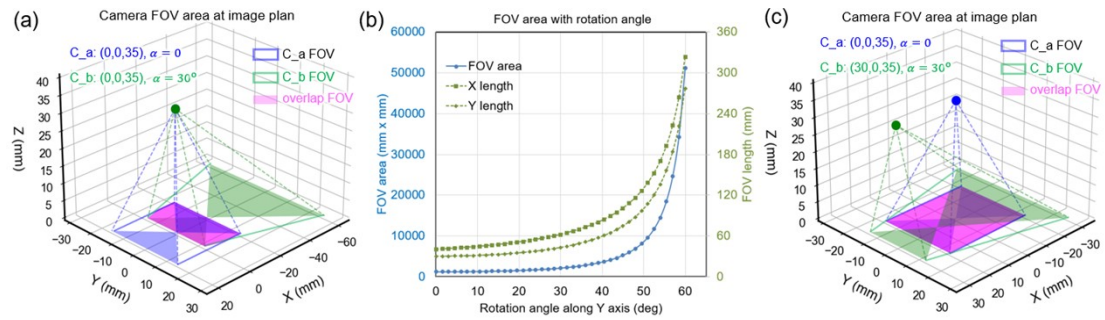


Figure S7. Observation of camera installed on the microfluidic chip. (a) Calculation of camera field of view, camera setting at (0,0,35), blue rectangle area, and rotating 30 degrees along with y-axis, green polygon area, magenta area is overlapping area. (b) Camera field of view and distance under different rotating angles along with y-axis. (c) Calculation of camera field of view, camera setting at (30,0,35) and rotating 30 degrees along with y-axis, green polygon area, magenta area is overlapping area.

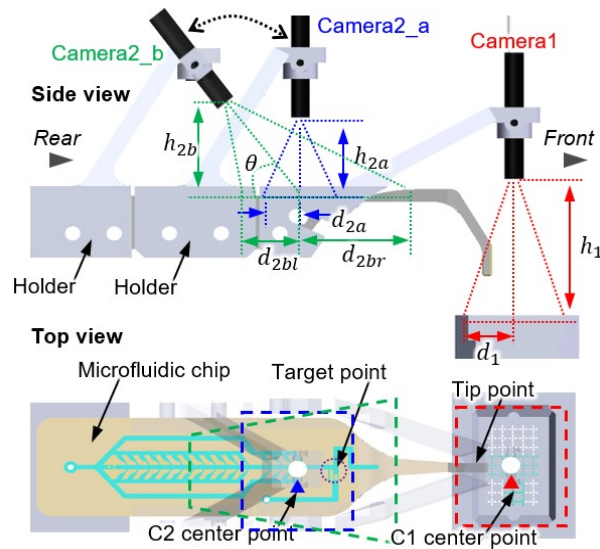


Figure S8. Scheme diagram of camera when camera 2 rotates.

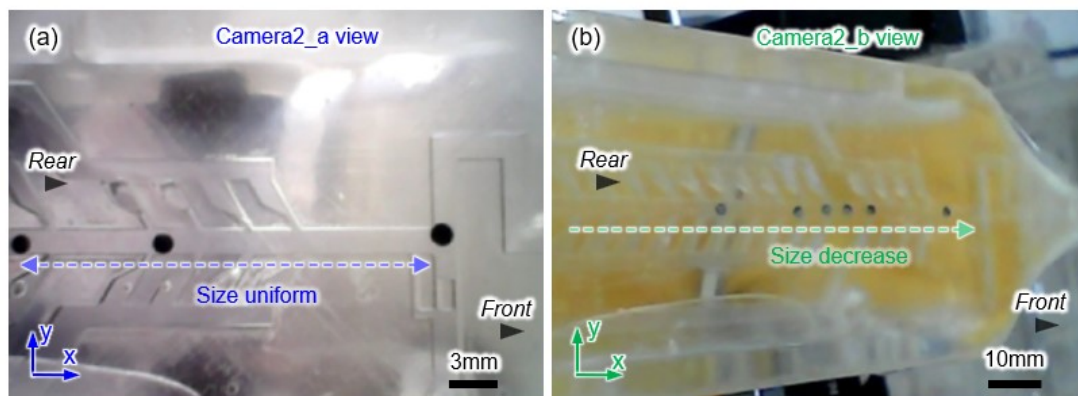


Figure S9. View effect of camera 2 installed at different position a (a) and position b (b).

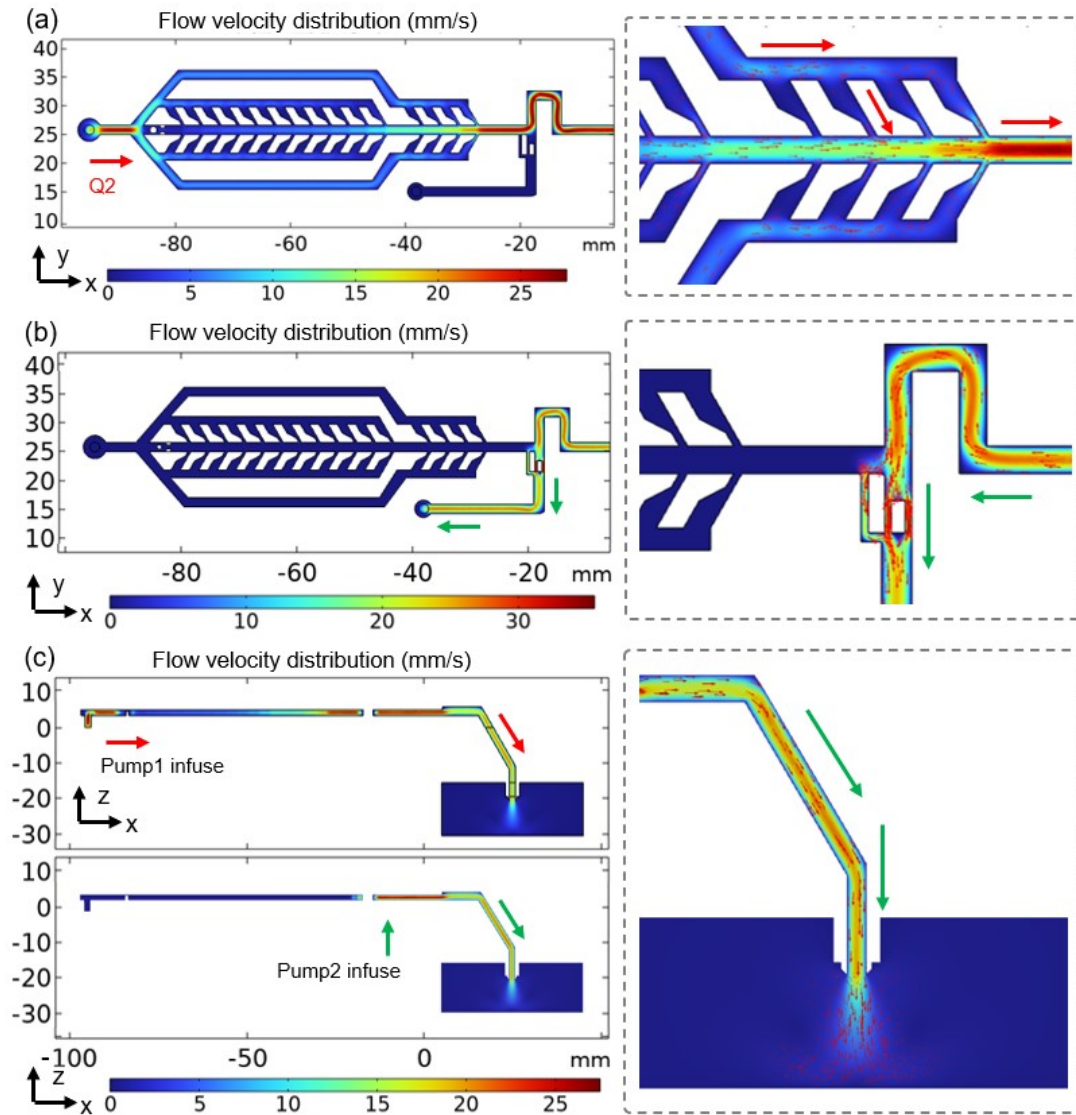


Figure S10. Simulation of flow distribution in the microfluidic chip. Flow velocity distribution with pump 1 infusing for separation oocytes (a) and pump 2 withdrawing for dealing with un-separated oocytes (b), $Q_2 = 2$ ml/min. (c) Flow velocity distribution with pump 1 and pump 2 infusing for placing oocytes.

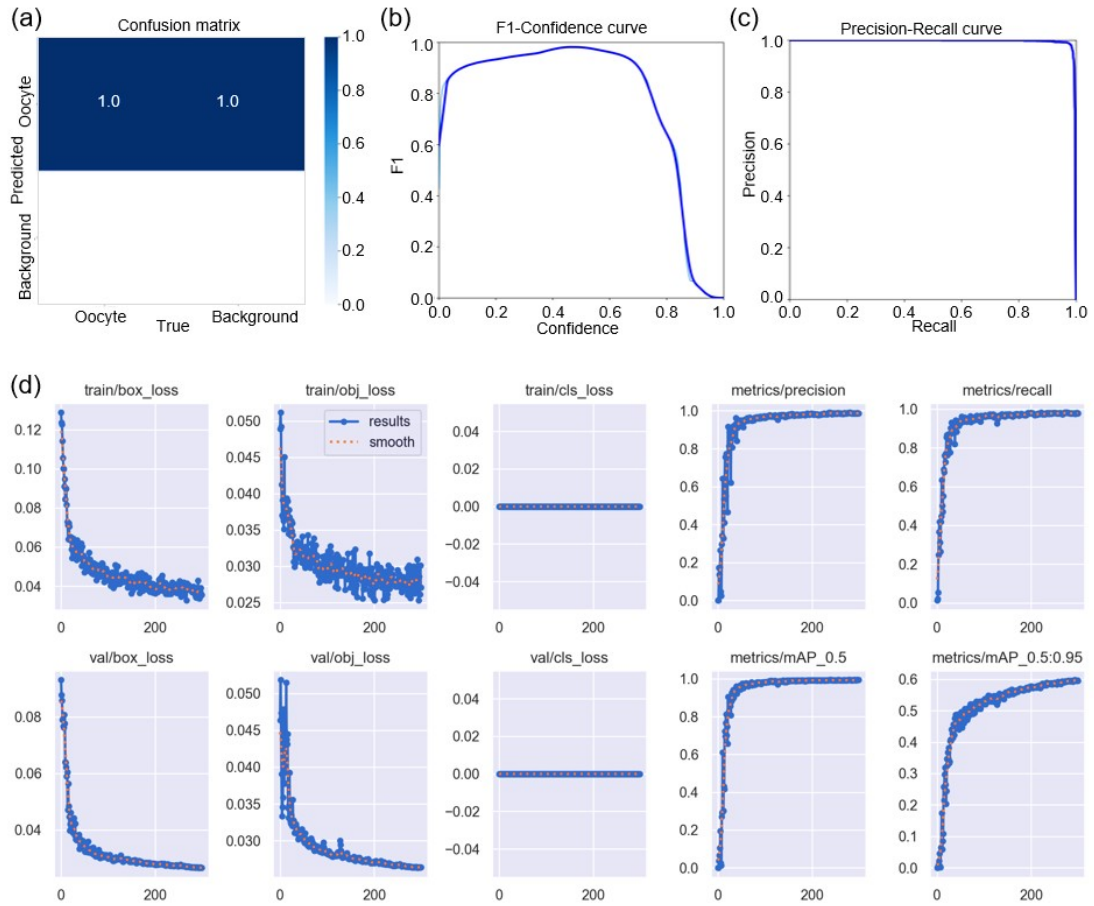


Figure S11. Training results of detection of oocytes by YOLOv5 model. (a) Confusion matrix. (b) F1-Confidence curve. (c) Precision-Recall curve. (d) Related loss and mAP results.

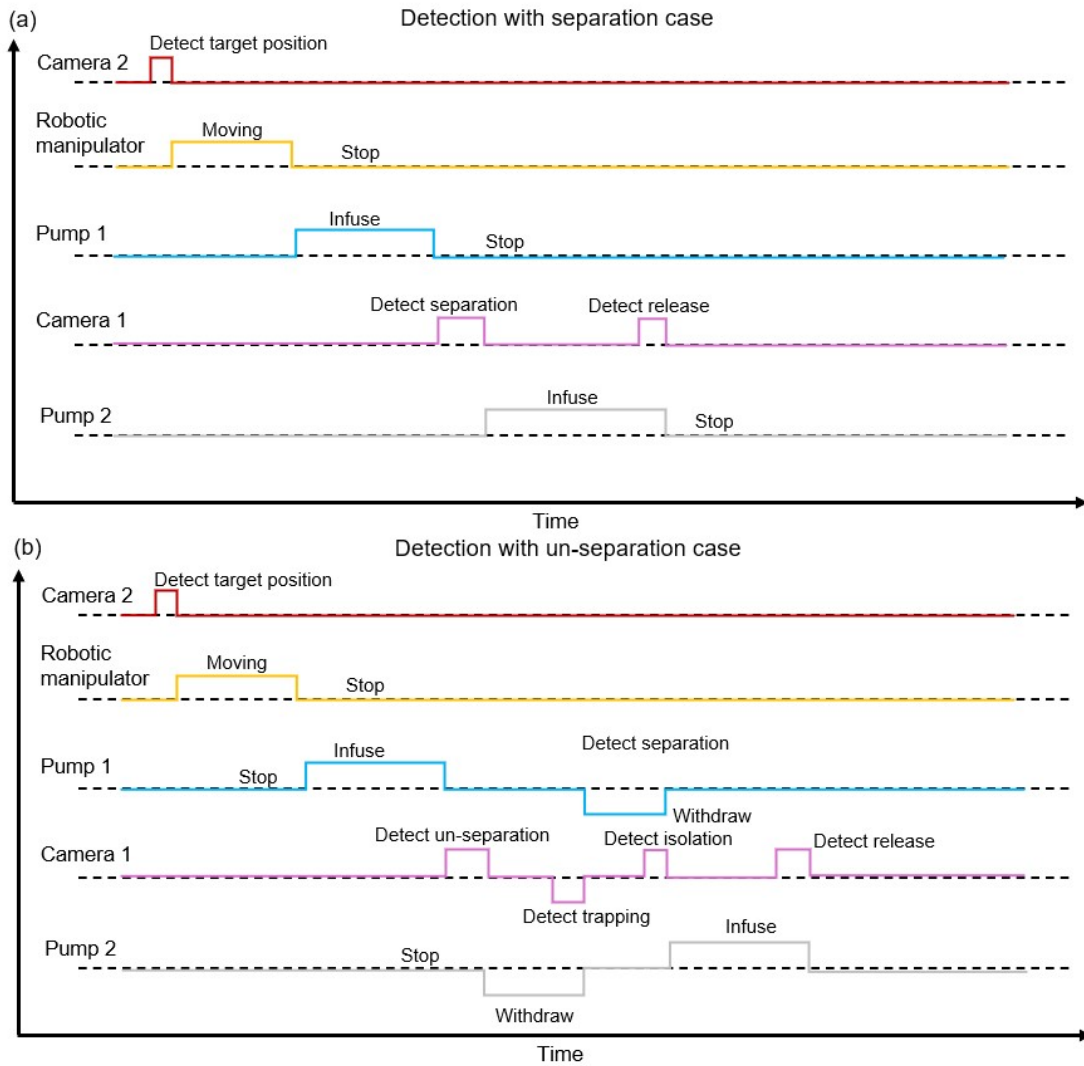


Figure S12. Timing control process of the system in (a) separation case and (b) un-separation case.

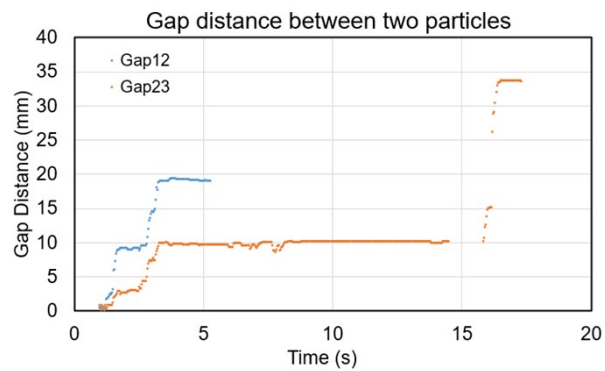


Figure S13. Gap distance between two adjacent objects.

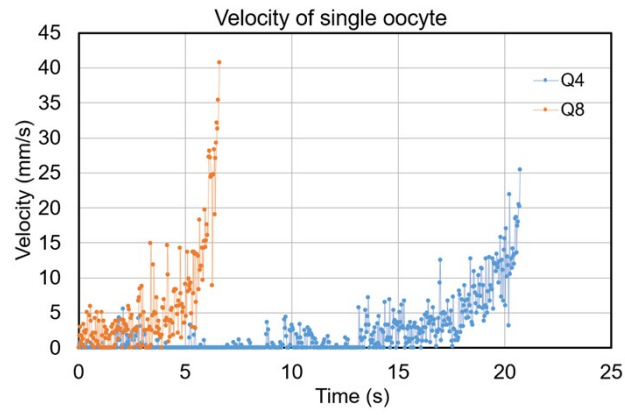


Figure S14. Velocity of objects in channel.

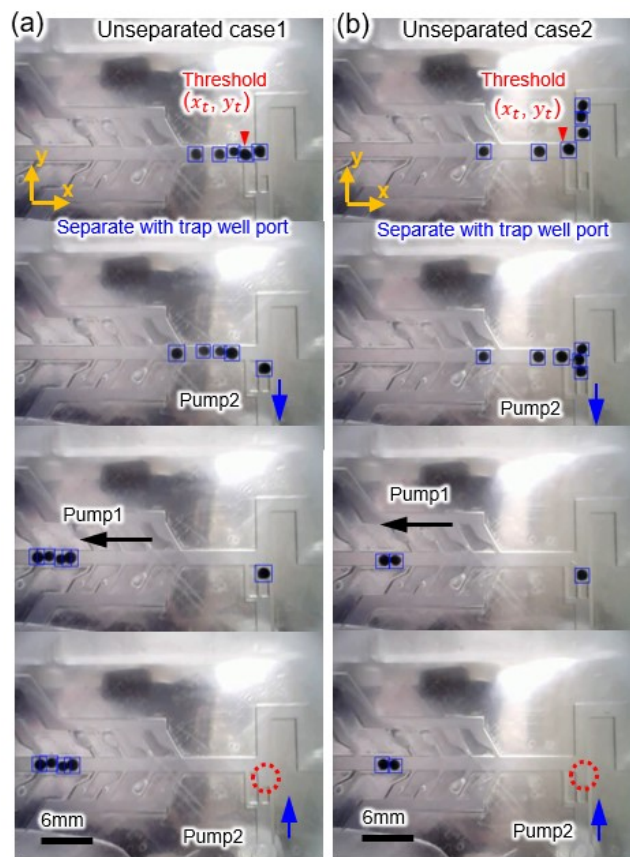


Figure S15. Dealing with unseparated cases with 2 hydrogel beads (1.2 mm) beyond threshold position (a) and more than 2 beads beyond threshold position, pump 2 withdraw for trapping single bead, switching to pump 1 withdraw remain beads, switching to pump 2 infuse for single bead release.

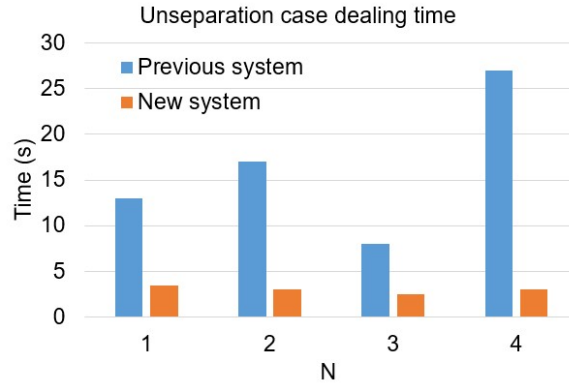


Figure S16. Processing time of un-separation case of oocyte in different system.

Rate (ml/min)	Pump 1 (+infuse, -withdraw)			
	+2	0	-2	
Pump 2	+2	Place	Place	No pick
	+1			Pick
	0	Place		Pick
	-1	Place		
	-2	NO place	Pick	Pick

Figure S17. Control flow of two pumps, orange and blue backgrounds are simulated items.

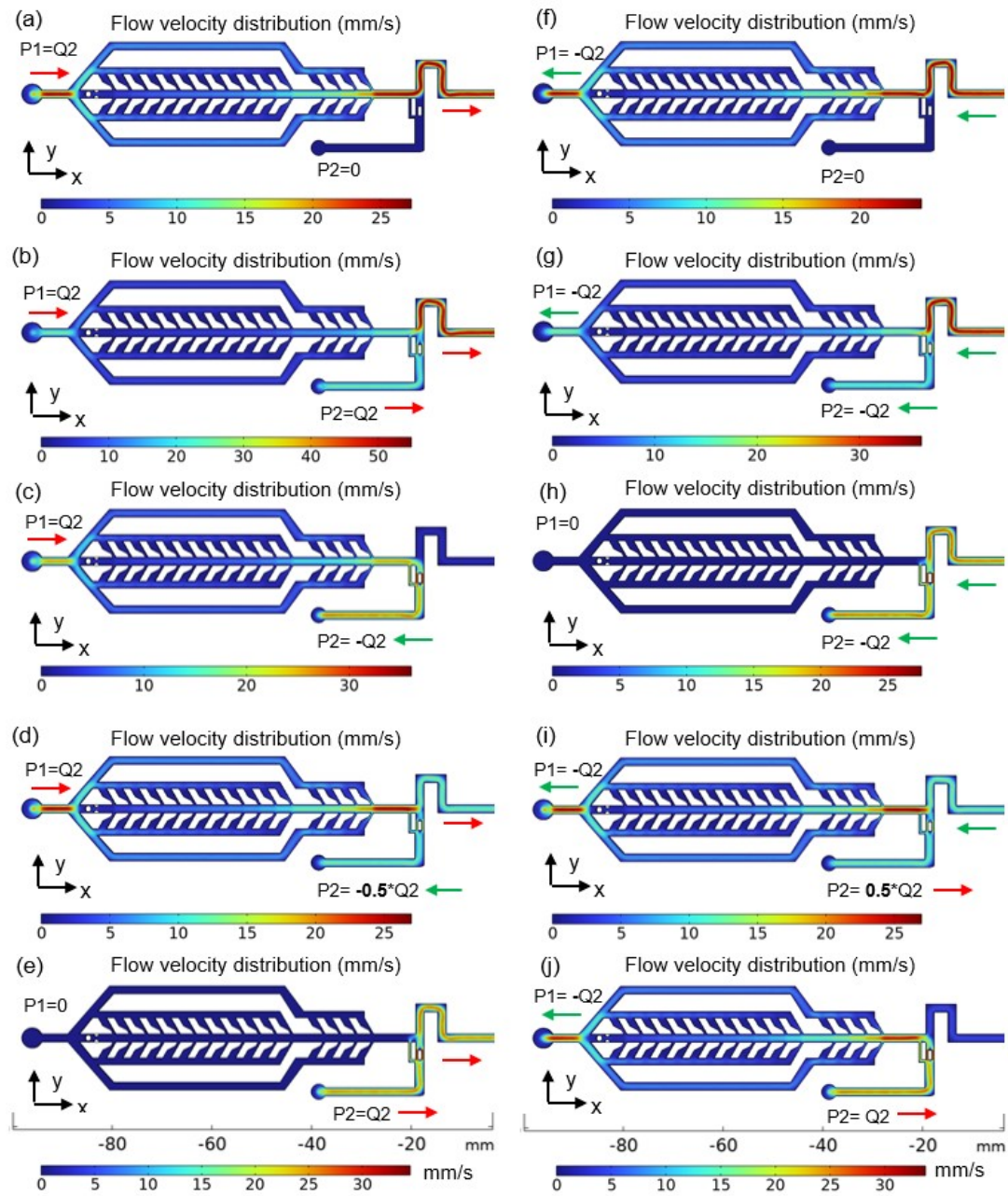


Figure S18. Flow distribution with different control state of two pumps for pick and place, $Q2 = 2$ ml/min. (a) $P1 = 2$ ml/min and $P2 = 0$. (b) $P1 = 2$ ml/min and $P2 = 2$ ml/min. (c) $P1 = 2$ ml/min and $P2 = -2$ ml/min. (d) $P1 = 2$ ml/min and $P2 = -1$ ml/min. (e) $P1 = 0$ and $P2 = 2$ ml/min. (f) $P1 = -2$ ml/min and $P2 = 0$. (g) $P1 = -2$ ml/min and $P2 = -2$ ml/min. (h) $P1 = 0$ and $P2 = -2$ ml/min. (i) $P1 = -2$ ml/min and $P2 = 1$ ml/min. (j) $P1 = -2$ ml/min and $P2 = 2$ ml/min.

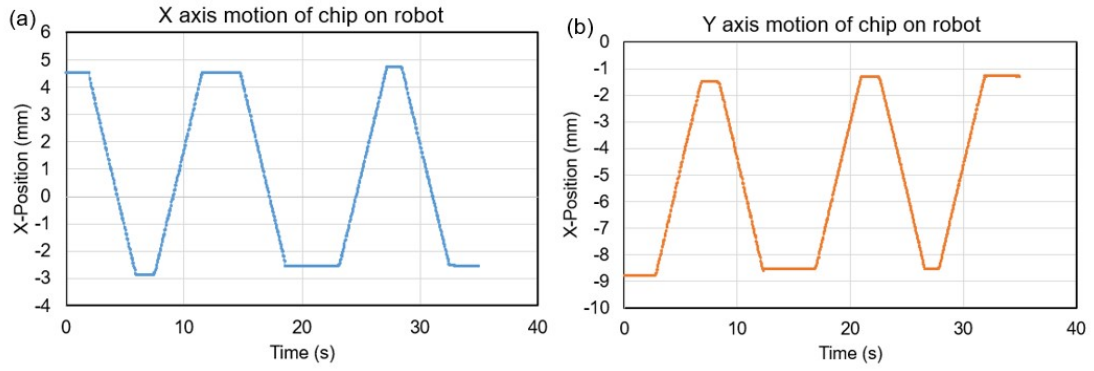


Figure S19. X axis (a) and Y axis (b) real motion, respectively.

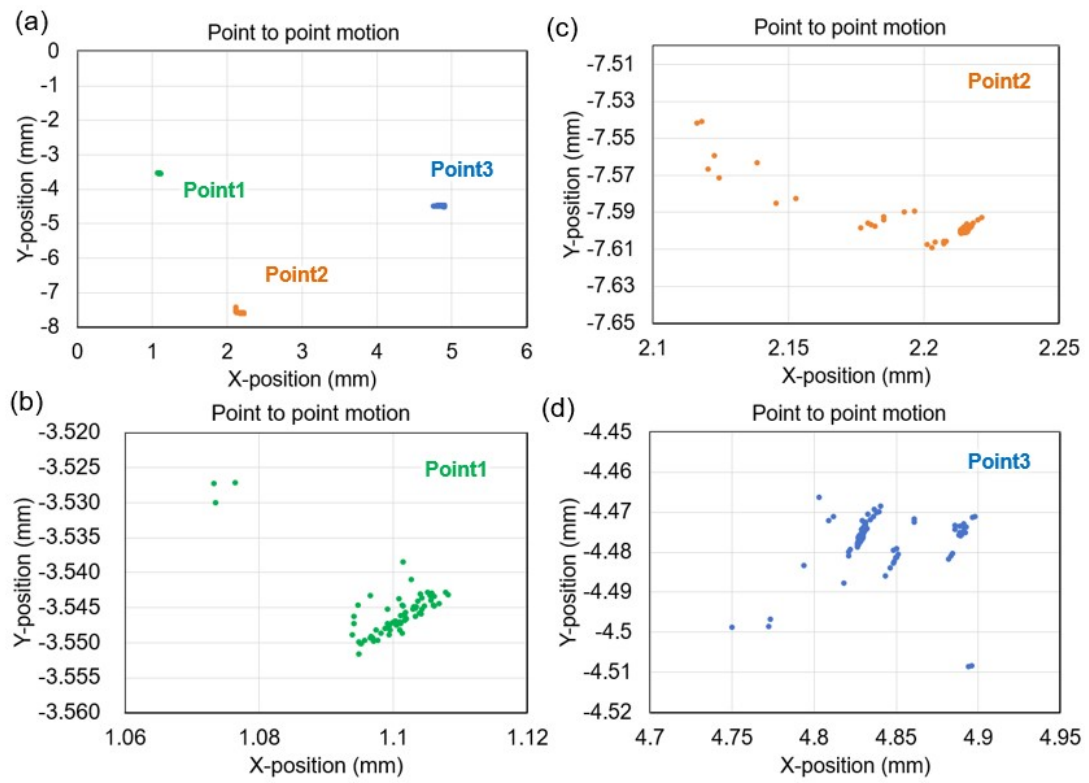


Figure S20. Motion of point to point. Repeatability of 3 points (a), point 1 (b), point 2 (c), and point 3 (d).